

# **PNEUMATICALLY ACTUATED EXOSKELETON FOR GAIT REHABILITATION**

Natasa Koceska\*, Saso Koceski\*, Pierluigi Beomonte Zobel\*\* and Francesco Durante\*\*

\*University “Goce Delce” – Stip, Faculty of Computer Science, Macedonia

\*\*University of L'Aquila, Applied Mechanics Laboratory DIMEG, Italy

## **ABSTRACT**

This paper describe the mechanical and control system design of a 10 DOF (Degrees Of Freedom) lower limbs exoskeleton for gait rehabilitation of patients with gait dysfunction. The system has 4 double-acting rod pneumatic actuators (two for each leg), that controls the hip and knee joints. Motion of each cylinder's piston is controlled by two pressure proportional valves, connected to both cylinder chambers. The pneumatic actuators are controlled by proportional-pressure valves. The control strategy has been specifically designed in order to ensure a proper position control guiding patient's legs along a fixed reference gait pattern. For this purposes Fuzzy controller with additional force compensator was developed. A numerical solution of the inverse kinematics problem based on video image analysis has been used. The controller was successively implemented and tested on embedded real-time PC104 system. Laboratory experiments without patient are carried out and the results are reported and discussed.

## **KEY WORDS**

Exoskeleton, fuzzy logic, rehabilitation robotic, treadmill training

## **INTRODUCTION**

Intensive training and exercise may enhance motor recovery or even restore motor function in people suffering from neurological injuries, such as spinal cord injury (SCI) and stroke. Repetitive practice strengthens neural connections involved in a motor task through reinforcement learning, and therefore enables the patients a faster and better re-learning of the locomotion (walking). Practice is most effective when it is task-specific [1],[2].

Thus, rehabilitation after neurological injury should emphasize repetitive, task-specific practice that promotes active neuromuscular recruitment in order to maximize motor recovery. Body-weight-supported treadmill training (BWSTT) is an emerging rehabilitation technique for gait

rehabilitation of patients with locomotor dysfunctions in the lower extremities. Clinical studies have confirmed that individuals who receive bodyweight supported treadmill training following stroke [3], [4] and spinal cord injury [5]-[7] demonstrate improved electromyographic (EMG) activity during locomotion [8], walk more symmetrically [9], are able to bear more weight on their legs. BWSTT involves practice of stepping on a motorized treadmill while unloading a percentage of a person's body weight using a special suspension system. Manual assistance, from 2 or 3 physiotherapists, is provided as necessary to promote upright posture and lower-extremity trajectories associated with normal human gait. For therapists this training is labor-intensive; therefore, training sessions tend to be short because of the physical demands on the therapists, which

may limit the full potential of the treatment. Also, manually assisted treadmill training lacks repeatability and objective measures of patient performance and progress.

A promising solution for assisting patients during rehabilitation process is to design exoskeleton devices. It has already been shown that robot-assistive devices can be very helpful in training individuals to regain their walking ability following incomplete spinal cord injury [10].

In the general setting of these robotic systems, a therapist is still responsible for the nonphysical interaction and observation of the patient by maintaining a supervisory role of the training, while the robot carries out the actual physical interaction with the patient.

Several groups are working on development of exoskeletal devices for “gait training”. Lokomat is a motorized exoskeleton that can drive hip and knee flexion through the four rotary joints driven by dc motors via precision ball screws [11]. Mechanized Gait Trainer (MGT) is a one degree-of-freedom powered machine that moves a patient’s legs in a gait-like pattern by driving two foot plates connected to a double crank and rocker system that is actuated by a motor via a planetary gear system [12]. AutoAmbulator is a rehabilitation machine for the leg to assist individuals with stroke and spinal cord injuries. PAM is a device that can assist the pelvic motion during stepping using BWST, and it’s used in combination with POGO- the pneumatically operated gait orthosis [13]. Most of these devices are using electric motors as actuators.

The rehabilitation robot system presented in this work is developed in the Laboratory of Applied Mechanics at DIMEG of University of L’Aquila and is pneumatically actuated. The pneumatic actuators have been adopted in this work as an alternative solution to the widely used electric motors, due to their large power output at a relatively low cost. They are also clean, easy to work with, and lightweight. Moreover, the choice of adopting the pneumatic actuators to actuate the joints is biologically inspired. They provide linear movements, and are actuated in both directions, so the articulation structures do not require the typical antagonistic scheme proper of the biological joints.

However, pneumatic systems exhibit highly non-linear behaviors which are associated with the compressibility of air, the complexity of friction presence and the nonlinearity of valves [14]-[15]. Because of all these characteristics, it is very difficult to successfully apply the classical control theory on pneumatic systems. It is relatively easier to use a fuzzy logic control, even though there are difficulties in designing a fuzzy controller and determining its parameters by trial and test.

Applying fuzzy control to a continuous pneumatic positioning system is particularly advantageous in terms of

simplicity of design and implementation, and thus significantly reduces the time required to develop the entire system [16]. Also fuzzy control has been demonstrated to provide highly satisfactory results in terms of accuracy, repeatability and insensitivity to changes in operating conditions [16].

This paper describes mechanical and control system design of the lower limbs exoskeleton for gait rehabilitation. Design choices for realization of the prototype are presented, the control architecture is described and experimental results, obtained without patient, are reported.

The evaluation of the system design and the proposed control architecture is foreseen in three experimental phases: experiments without patient, experiments with voluntary healthy patients and finally tests on disable persons.

## EXOSKELETON STRUCTURE

Designing an exoskeleton device for functional training of lower limbs is a very challenging task. From an engineering perspective, the designs must be flexible to allow both upper and lower body motions, once a subject is in the exoskeleton, since walking involves synergy between upper and lower body motions. It must be also a light weight, easy wearable and must guarantee comfort and safety. From a neuro-motor perspective, an exoskeleton must be adjustable to anatomical parameters of a subject.

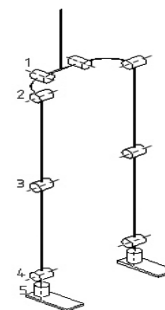


Fig.1. DOFs of the exoskeleton

Considering these characteristics an exoskeleton structure with 10 rotational DOF was studied and realized. An optimal set of DOF was chosen after studying the literature on gait, and in order to allow for subject to walk normally and safely in the device.

The degrees of freedom, all rotational, are: the number 1 with axis perpendicular to the front, the numbers 2, 3 and 4 with axes perpendicular to the sagittal plane, the number 5 with axis perpendicular to the ground; of these only DOF 2 and 3 are motorized (Fig.1).The robot moves in parallel to the skeleton of the patient, so that no additional DOF or

motion ranges are needed to follow the patient motion. The mechanical structure of the shapes and the dimensions of the parts composing the exoskeleton are human inspired and have an ergonomic design.

The inferior limbs of the exoskeleton are made up of three links corresponding to the thighbone, the shinbone and the foot. The thighbone link is 463 mm long and has a mass of 0.5 kg and the shinbone link is 449 mm long and has a mass of 0.44 kg.

The prototype structure is adjustable to the patients which are tall from 175 cm up to 190 cm without any functional problems (Fig. 2a, 2b). For better wearability of the exoskeleton an adjustable connection between the corset of polyethylene (worn by the patient) and the horizontal rod placed at the pelvis level is provided. Moving the exoskeleton structure up for only 25 mm, the distance between the centre of the knee joint and the vertical axes of the hip articulation, is reduced to 148 mm (Fig.2c), while the corset remains in the same position.

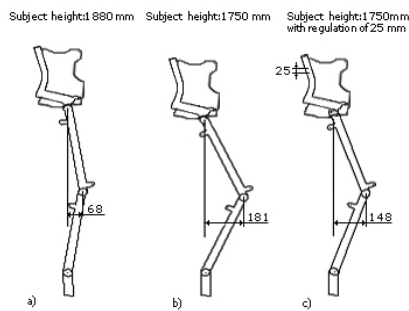


Fig.2. Adjustability of the realized prototype

In order to realize a prototype with anthropomorphic structure that will follow the natural shape of the human's lower limbs, the orientation and position of the human leg segments were analyzed. In the case of maximum inclination, the angle formed by the vertical axis and a leg rod is  $2.6^\circ$ , observed in frontal plane (Fig.3). The inclination of  $1.1^\circ$  was chosen for the stand position, while other  $1.5^\circ$  are given by a lateral displacement of 30 mm, when the banking movement occurs.

In this way the ankle joint is a little bit moved towards the interior side with respect to the hip joint, following the natural profile of the inferior limbs in which the femur is slightly oblique and form an angle of  $9^\circ$  with the vertical while for the total leg this angle is reduced to  $3^\circ$ . The other actuator which moves the knee joint is connected bellow the shinbone and has a rod stroke of 160 mm.

Both actuators are with bore diameter of 32 mm, capable to provide force of about 700 N under a supply pressure of 0.9 MPa coming by the external compressor (Fig.4).The motion of each cylinder's piston (i.e. supply and discharge of both

cylinder chambers) is controlled by two pressure proportional valves (SMC-ITV 1051-312CS3-Q), connected to both cylinder chambers.

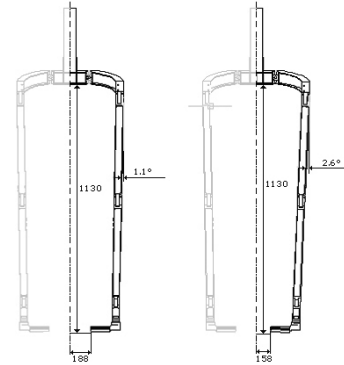


Fig.3. Positioning of the exoskeleton shinbone and thighbone link, realized following the human leg position



Fig.4. Mechanical structure of the exoskeleton with pneumatic actuators

The selection of the valve was due to the primary calculations for air flow through the valve. Each valve controls only one chamber of the actuator, therefore the calculations of the air flow is made only in one phase of the actuators cycle. Simulations done in Working Model 2D software showed that the outgoing speed of a piston ( $v$ ) is 50 mm/s, which occurs during the pre-swing phase of the walking cycle when a force of about 700 N is required. As said before this force will be provided by a cylinder chamber's pressure of 0.9 MPa (relative).

The selected valve model satisfies these requirements. The exoskeleton structure also has to guarantee the safety of the patient. As the joints motions of the robot directly correspond with that of a patient, it was relatively easy to implement the mechanical safety limits (physical stops), which are placed on extreme ends of the allowed range of motion of each DOF. For hip and knee joints in the sagittal plane, the stops can withstand the maximum torque that the

actuators can apply. The structure of the exoskeleton is realized in aluminum which ensures a light weight and a good resistance.

In order to calculate the mechanical resistance, all exoskeleton components are imported in Visual Nastran, where Finite Element Analysis (FEA) was done.

The stresses measured (Von Mises stresses) are well below the yield strength of aluminum 6082 T6 ( $\sigma_y = 200$  MPa) chosen as the material for realization of the exoskeleton.

Hip and knee angles, of our rehabilitation system, are acquired with the rotational potentiometers.

The overall exoskeleton structure is positioned on a treadmill and supported, at the pelvis level, with a space guide mechanism that allows vertical and horizontal movements. Space guide mechanism is connected with the chassis equipped with a weight balance system (Fig.5).



Fig. 5. Realized prototype of the overall rehabilitation system

## KINEMATIC AND STATIC ANALYSIS

In the present section, the joints excursions have been analyzed for each articulation, making particular attention to the related actuators extensions and the forces they have to provide in order to move the articulations.

### A. Knee articulation

In order to characterize the joint kinetic behavior, it is useful to analyze the actuator force necessary to counteract the gravitational load acting on the shinbone center of mass, varying the knee joint angular position. The knee articulation realized has only one DOF and thus it is actuated by only one pneumatic actuator as it can be seen on Fig.4. The knee articulation scheme is shown on the Fig.6a.

The  $p$  segment represents the pneumatic actuator, whereas the knee angle position is indicated by the  $\theta$  angle.

The direct kinematic problem is easy to solve. In a few words, the process calculates the actuator length once known the rotation angle  $\theta$ .

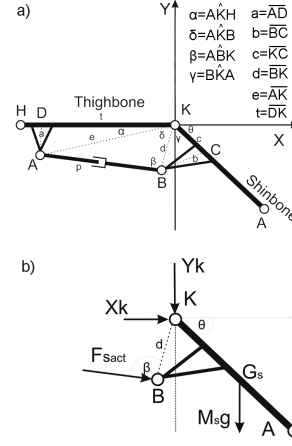


Fig. 6. a) Knee articulation scheme and b) free body diagram of the shinbone

The equations (1) show this process, considering the geometrical structure and the connections between different components.

$$\begin{cases} \gamma = \cos^{-1}\left(\frac{d^2 + c^2 - b^2}{2dc}\right) \\ \alpha = \cos^{-1}\left(\frac{t^2 + e^2 - a^2}{2te}\right) \\ \delta = \pi - \theta - \gamma - \alpha \\ p = \sqrt{e^2 + d^2 - 2ed \cos \delta} \end{cases} \quad (1)$$

After the calculation of the actuators length  $p$ , the angle  $\beta$  can be easily deduced as in (3):

$$\beta = \sin^{-1}\left(\frac{e \sin \delta}{p}\right) \quad (2)$$

$F_{Sact}$  represents the force supplied by the shinbone pneumatic actuator, whereas the arrow indicated by  $M_{Sg}$  shows the opponent force caused by the gravity.  $M_S$  is the approximate sum of the mass of the shinbone and the foot applied in the center of mass of the shinbone. Moreover, the segment  $d$  represents the arm of the cylinder force.

From a simple torque balance with respect to the point K, Fig. 6b, the relation between  $F_{Sact}$  and the knee angular position  $\theta$  is derived as in (3).

$$F_{Sact} = \frac{M_S g L_{KG_s} \cos(\theta)}{d \sin(\beta)} \quad (3)$$

From (1), (2) and (3) it can be seen that the force supplied by the shinbone pneumatic actuator can be expressed as a

function of the  $\theta$  angle, obtained by the knee rotational potentiometer.

### B. Hip articulation

As the knee articulation also the hip articulation of our prototype has only one DOF and thus is actuated by only one pneumatic actuator as it can be seen on Fig.4. The hip articulation scheme is shown on the Fig.7a.

Analyzing the hip articulation torque, one can observe that the rod of the thighbone pneumatic actuator is connected to the segment c placed upon the thighbone. In particular, the segment b in this case, represents the arm on which the hip joint force acts.

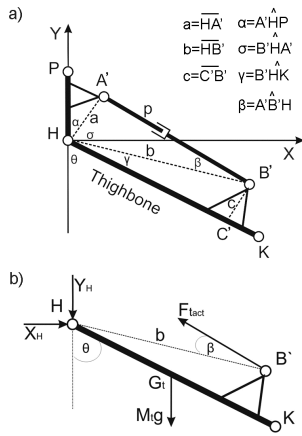


Fig. 7. a) Hip articulation scheme and b) free body diagram of the thighbone

The kinematic problem for this actuator, i.e. the process that calculates the actuator length knowing the rotation angle  $\theta$ , is described with (4).

For a certain actuator length  $p$ , the angle  $\beta$  can be easily deduced as in (5).  $F_{Tact}$  indicates the force supplied by the thighbone pneumatic actuator, whereas the arrow indicated by  $M_T g$  shows the opponent force caused by the gravity.  $M_T$  is the approximate sum of the weights of the thighbone, shinbone and the foot applied in the center of mass of the thighbone.

$$\begin{cases} \gamma = \cos^{-1} \left( \frac{b^2 + L_{HC'}^2 - c^2}{2bL_{HC'}} \right) \\ \sigma = \pi - \gamma - \alpha - \theta \\ p = \sqrt{a^2 + b^2 - 2ab \cos \sigma} \end{cases} \quad (4)$$

$$\beta = \sin^{-1} \left( \frac{a \sin \sigma}{p} \right) \quad (5)$$

From a simple torque balance Fig. 7b, the  $F_{Tact}$  value depending of the hip angular position is derived. Equation (6) shows the relation found for the hip articulation.

$$F_{Tact} = \frac{M_T g L_{HC'} \sin \theta}{b \sin \beta} \quad (6)$$

From (4), (5) and (6) it can be seen that the force supplied by the thighbone pneumatic actuator also can be expressed as a function of the  $\theta$  angle obtained by the hip rotational potentiometer.

So, analytic relations between the forces provided by the pneumatic actuators and the torques needed to move the hip and knee articulations have been found. In particular, in our case it is useful to analyze the forces necessary to counteract the gravitational load acting on the thighbone and shinbone center of mass, varying the joints angular position, because it offers the possibility of inserting a further compensation step in the control architecture in order to compensate the influence of the torques during the movement.

### INVERSE KINEMATIC PROBLEM

To analyze the human walking, a camera based motion captured system was used. Motion capturing of a healthy subject walking on the treadmill, was done with one video camera placed with optical axis perpendicular in respect of the sagittal plane of the gait motion. The subject had markers mounted on hip, knee and ankle. An object with known dimensions (grid) was placed inside the filming zone, and it was used like reference to transform the measurement from pixel to the distance measurement unit. The video was taken with the resolution of 25 frame/s.

The recorded video was post-processed and kinematics parameters of limbs' characteristic points (hip, knee and ankle) were extracted.

After that, the obtained trajectory was used to resolve the problem of inverse kinematics of the lower limb rehabilitation system. The inverse kinematic problem was resolved in numerical way, with the help of Working Model 2D software. By the means of this software the target trajectory, which should be performed by each of the actuators, was determined.

### FUZZY CONTROLLER

Fuzzy logic is basically a rule-based operation, in "if <condition> then <operation>". Compared with the traditional rule-based method, the condition and operation are fuzzy descriptions in a fuzzy controller. Thus the measured information is interpreted to fuzzy descriptions through the membership function. The output control signal

is calculated from the operation by a defuzzification processing. Fuzzy control emulates human control strategy, and its principle is easy to understand.

The state variables of the pneumatic fuzzy control system are: the actuator length error E, which is the input signal and two output control signals  $U_{rear}$  and  $U_{front}$  which are control voltages of the valves connected to the rear chamber and front chamber respectively.

Actuator length error in the system is given by:

$$E(kT) = R(kT) - L(kT) \quad (7)$$

where,  $R(kT)$  is the target displacement,  $L(kT)$  is the actual measured displacement, and  $T$  is the sampling time.

Based on this error the output voltage, that controls the pressure in both chambers of the cylinders, is adjusted.

Seven linguistic values non-uniformly distributed along their universe of discourse have been defined for input/output variables (negative large-NL, negative medium-NM, negative small-NS, zero-Z, positive small-PS, positive medium-PM, and positive large-PL). For this study trapezoidal and triangular-shaped fuzzy sets are chosen for input variable and singleton fuzzy sets for output variables.

The membership functions were optimized starting from a first, perfectly symmetrical set. Optimization was performed experimentally by trial and test with different membership function sets. The membership functions that give optimum results are illustrated in Figs. 8, 9 and 10.

The rules of the fuzzy algorithm are shown in Table I in a matrix format. The max-min algorithm is applied and center of gravity (CoG) method is used for defuzzify and to obtain an accurate control signal.

Since the working area of cylinders is overlapping, the same fuzzy controller is used for both of them.

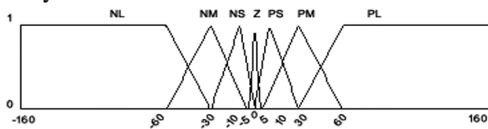


Fig. 8. Membership functions of input variable E

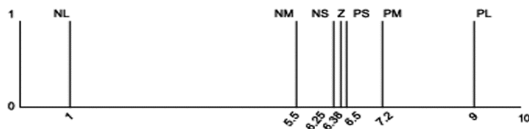


Fig. 9. Membership functions of output variable  $U_{front}$

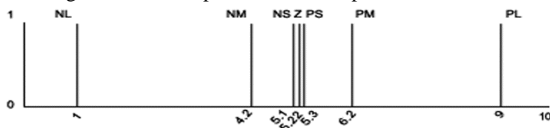


Fig. 10. Membership functions of output variable  $U_{rear}$

Rule n °	E	ANT	POS
1	PL	PL	NL
2	PM	PM	NM
3	PS	PS	NS
4	Z	Z	Z
5	NS	NS	PS
6	NM	NM	PM
7	NL	NL	PL

Table 1 Rule matrix of fuzzy controller

## CONTROL ARCHITECTURE

The overall control architecture is presented on the Fig.11. In particular, it is based on fuzzy logic controllers which aim to regulate the lengths of thighbone and shinbone pneumatic actuators, described in *Fuzzy controller* Section.

The force compensators are calculating the forces necessary to counteract the gravitational load acting on the thighbone and shinbone center of mass, varying the joints angular position.

Target pneumatic actuators lengths obtained by off-line procedure described in the *Inverse kinematic problem* Section were placed in the input data module. In this way there is no necessity of real-time calculation of the inverse kinematics and the complexity of the overall control algorithm is very low.

The feedback information is represented by the hip and knee joint working angles and the cylinder lengths, calculated according to (2) and (5).

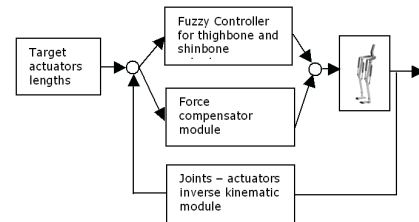


Fig. 11. Control architecture diagram

The global control algorithm runs inside an embedded PC104, which represents the system supervisor. The PC104 is based on Athena board from Diamond Systems, with real time Windows CE.Net operating system, which uses the RAM based file system. The Athena board combines the low-power Pentium-III class VIA Eden processor (running at 400 MHz) with on-board 128 MB RAM memory, 4 USB ports, 4 serial ports, and a 16-bit low-noise data acquisition circuit, into a new compact form factor measuring only 4.2" x 4.5". The data acquisition circuit provides high-accuracy; stable 16-bit A/D performance with 100 KHz sample rate,

wide input voltage capability up to +/- 10V, and programmable input ranges. It includes 4 12-bit D/A channels, 24 programmable digital I/O lines, and two programmable counter/timers. A/D operation is enhanced by on-board FIFO with interrupt-based transfers, internal/external A/D triggering, and on-board A/D sample rate clock.

The PC 104 is directly connected to each rotational potentiometer and valves placed onboard the robot.

In order to decrease the computational load and to increase the real-time performances of the control algorithm the whole fuzzy controller was substituted with a hash table with interpolated values and loaded in the operating memory of the PC104.

## EXPERIMENTAL RESULTS

To evaluate the performance of the exoskeleton structure together with the proposed control architecture experimental tests without patients were performed.

The experiments were conducted with a sampling frequency of 10 Hz, and a pressure of 0.6 MPa.

The movement was natural and smooth while the limb moves along the target trajectory.

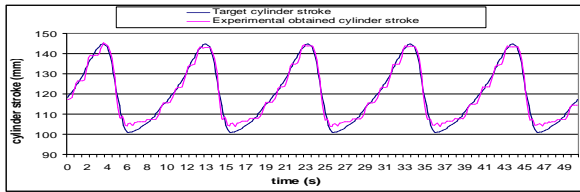


Fig. 12. Target and experimentally obtained thighbone actuator stroke during the gait cycle

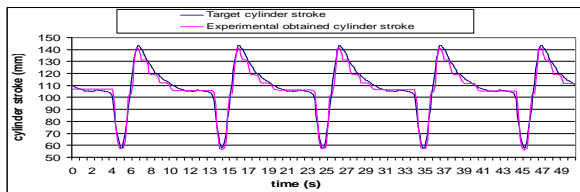


Fig. 13. Target and experimentally obtained shinbone actuator stroke during the gait cycle

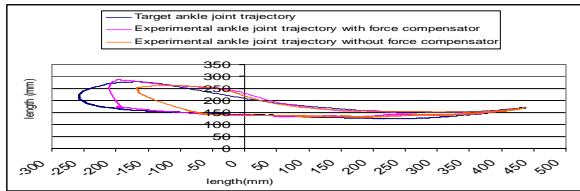


Fig. 14. Ankle joint trajectory (target, experimental without force compensator and experimental with force compensator)

Fig.12 and Fig.13 show the target and experimentally obtained stroke for thighbone and shinbone actuators, respectively.

As it can be observed from the graphs, the cylinders tracked the target trajectory well with the max. error of 5mm for the thighbone actuator, and 6mm for the shinbone actuator, which is accurate enough for the desired purpose. Results for the target and experimental ankle joint trajectory, for one cycle, with and without implementation of the force compensator, are shown in Fig.14.

From the graph we can observe that there is significant improvement of the gait trajectory when a force compensator is used.

During the gait training one of the most important goals to achieve is path repeatability. In order to test the path repeatability, ISO 9283 standard was used. According to this standard path repeatability expresses the closeness of the agreement between the attained paths for the same command path followed n times in the same direction. Path repeatability is expressed by  $RT_p$ -the maximum  $RT_{pi}$  which is equal to the radius of a circle in the normal plane and with its centre on the barycentre line (Fig. 15).

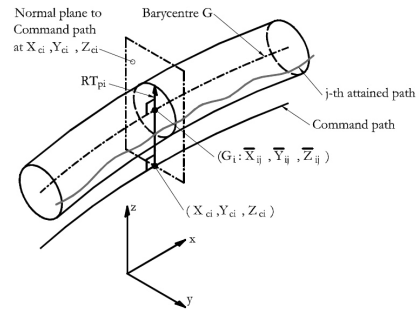


Fig. 15. Target and experimentally obtained thighbone actuator length during the gait cycle (RT represent repeatability; G represents the barycentre of a cluster of attained poses;  $X_{ci}$ ,  $Y_{ci}$  and  $Z_{ci}$  are the coordinates of the  $i$ -th point of the command path;  $X_{ij}$ ,  $Y_{ij}$  and  $Z_{ij}$  are the coordinates of the intersection  $j$ -th attained path and the  $i$ -th normal plane)

The path repeatability is calculated as follow:

$$RT_p = \max RT_{pi} = \max[\bar{l}_i + 3S_{li}] ; i = 1 \dots m \quad (8)$$

where:

$$\bar{l}_i = \frac{1}{n} \sum_{j=1}^n l_{ij} \quad (9)$$

$$S_{li} = \sqrt{\frac{\sum_{j=1}^n (l_{ij} - \bar{l}_i)^2}{n-1}} \quad (10)$$

$$l_{ij} = \sqrt{(x_{ij} - \bar{x}_i)^2 + (y_{ij} - \bar{y}_i)^2 + (z_{ij} - \bar{z}_i)^2} \quad (11)$$

$$\bar{x}_i = \frac{1}{n} \sum_{j=1}^n x_{ij}; \quad \bar{y}_i = \frac{1}{n} \sum_{j=1}^n y_{ij}; \quad \bar{z}_i = \frac{1}{n} \sum_{j=1}^n z_{ij} \quad (12)$$

m is number of calculated points along the path, and n is number of measurement cycles.

Ten tests, with ten cycles, without load (the only load was the weigh of the exoskeleton structure), for the same command path, were conducted. The values for path repeatability were calculated and the corresponding results for all tests are shown in Table 2.

1	2	3	4	5	6	7	8	9	10
13.9	11.9	7.4	13.6	9.1	10.4	13.4	10.1	12.5	11.1

Table 2 Repeatability results (second row [mm])

Analyzing the results form Table 2, we can say that the path repeatability of our robot rehabilitation system is satisfactory.

## CONCLUSION

Powered exoskeleton device for gait rehabilitation has been designed and realized, together with proper control architecture. Its DOFs allow free leg motion, while the patient walks on a treadmill with its weight, completely or partially supported by the suspension system.

The use of pneumatic actuators for actuation of this rehabilitation system is reasonable, because they offer high force output, good backdrivability, and good position and force control, at a relatively low cost.

The control strategy was designed to ensure that the patient's legs will be guided along a fixed reference gait pattern. The inverse kinematic problem was solved in a numerical way and fuzzy controller used to regulate the lengths of thighbone and shinbone pneumatic actuators was developed. Additional compensation module to eliminate the influence of the torques during the movement was added.

The effectiveness of proposed control architecture was confirmed by experiments. The experimental results show that the developed control architecture can be considered an appropriate option for the control of the developed prototype.

In order to increase the performance of this rehabilitation system a force control loop should be implemented as a future development. The future work also foresees two more steps of evaluation of the system: experiments with voluntary healthy persons and experiments with disable patients.

## REFERENCES

1. F.M. Henry: Specificity vs. generality in learning motor skill, in *Classical Studies on Physical Activity*, R.C. Brown and G.S. Kenyon Ed. Englewood Cliffs, N.J., Prentice-Hall; 1968:331-340;
2. V.R. Edgerton, R.D. de Leon, N. Tillakaratne, M.R. Recktenwald, J.A. Hodgson, R.R. Roy: "Use-dependent plasticity in spinal stepping and standing," *Advances in Neurology* 1997, 72:233-247.
3. S. Hesse, C. Bertelt, A. Schaffrin, M. Malezic, and K. Mauritz, "Restoration of gait in non-ambulatory hemiparetic patients by treadmill training with partial body weight support," *Arch. Phys. Med. Rehabil.* 75, 1087-1093, October 1994.
4. S. Hesse, et al., "Treadmill training with partial body weight support: influence of body weight release on the gait of hemiparetic patients," *J. Neurol. Rehabil.* 11, 15-20, 1997.
5. A. Wernig, and S. Muller, "Laufband locomotion with body weight support improved walking in persons with severe spinal cord injuries," *Paraplegia* 30, 229-238, 1992.
6. A. Wernig, A. Nanassy, and A. Muller, "Laufband (treadmill) therapy in incomplete paraplegia and tetraplegia," *J. Neurotrauma* 16, 719-726, 1999.
7. V. Dietz, G. Colombo, L. Jensen, and L. Baumgartner, "Locomotor capacity of spinal cord in paraplegic patients," *Ann. Neurol.* vol. 37, no. 5, 574-582, May 1995.
8. M. Visintin, H. Barbeau, N. Bitensky, and N. Mayo, "Using a new approach to retrain gait in stroke patients through body weight support and treadmill training," *Stroke* 29,1122-1128, 1998.
9. E. Hassid, D. Rose, J. Commisarow, M. Guttry, and B. Dobkin, "Improved gait symmetry in hemiparetic stroke patients induced during body weight supported treadmill stepping," *J. Neurol. Rehabil.* 11, 21-26, 1997.
10. T.Hornby, D.Zemon and D. Campbell, "Robotic-assisted, body-weight-supported treadmill training in individuals following motor incomplete spinal cord injuri," *Physical Therapy*, vol. 85, no. 1, 52-66, Jan. 2005.
11. S. Jezernik, G. Colombo, T. Keller, H. Frueh, and M. Morari, "Robotic orthosis lokomat: A rehabilitation and research tool," *Neuromodulation*, vol. 6, no. 2, pp. 108-115, Apr. 2003.
12. S. Hesse and D. Uhlenbrock, "A mechanized gait trainer for restoration of gait," *J. Rehabil. Res. Development*, vol. 37, no. 6, pp. 701-708, 2000.
13. Daisuke Aoyagi, Wade E. Ichinose, Susan J. Harkema, David J. Reinkensmeyer, and James E. Bobrow, "A Robot and Control Algorithm That Can Synchronously Assist in Naturalistic Motion During Body-Weight-Supported Gait Training Following Neurologic Injury," *IEEE Transactions on neural systems and rehabilitation engineering*, vol.15, no. 3, Sep. 2007.
14. J. Y. Lai, C. H. Meng, and R. Singh, "Accurate position control of a pneumatic actuator," *Transactions of the ASME, Journal of Dynamic Systems, Measurement, and Control*, 112, 734-739, 1990.
15. J. Pu, R. H. Weston, and P. R. Moore, "Digital motion control and profile planning for pneumatic servos," *Transactions of the ASME, Journal of Dynamic Systems, Measurement, and Control*, 114, 634-640, 1992.
16. T.Raparelli, M.Velardocchia, P.Beomonte Zobel, "I controlli Fuzzy nella pneumatica", *I° Conv. Int. Trasmissioni di Potenza*, Milano, 20-21 giugno 1995, pp. 621-634.